



Determination of Combustion Kinetic Data of Some Agricultural Wastes from the Galicia-Northern Portugal Euroregion

Simão Mateus¹ · Victor Ferreira¹ · Aida Sanches¹ · Pedro Resende² · Carlos Pinho³

Received: 21 April 2020 / Accepted: 3 September 2020 / Published online: 11 September 2020
© Springer Nature B.V. 2020

Abstract

This work concerns the study of the combustion kinetic characteristics of chars made from three different biomass species, vine and kiwi pruning wastes, and gorse from forest cleaning process in a fluidized bed combustor, operating in the bubbling bed regime, at four bed temperatures, 750, 820, 850 and 920 °C. Batches of the original biomass pellets were carbonized in a nitrogen fluidized bed, either at 900 °C, for the kiwi and vine pellets, or at 800 °C for the gorse pellets. To acquire complete information on the combustion behaviour, different sizes of the char particles were subsequently burned in a bubbling fluidized bed. The evolution of the overall combustion resistance, and information on the combustion control were obtained. It was observed that for the kiwi and vine chars, the combustion was controlled through a combination of diffusion and kinetics, while for the gorse char the combustion was diffusionaly controlled. In addition, the pre-exponential factors and activation energies were obtained for the kiwi and vine chars, by applying the Arrhenius law to the kinetic data for each char. Activation energy values of 246.16 kJ/mol for the kiwi char and of 155.02 kJ/mol for the vine char were obtained.

✉ Carlos Pinho
ctp@fe.up.pt

Simão Mateus
smateus@inegi.up.pt

Victor Ferreira
vferreira@inegi.up.pt

Aida Sanches
asanches@inegi.up.pt

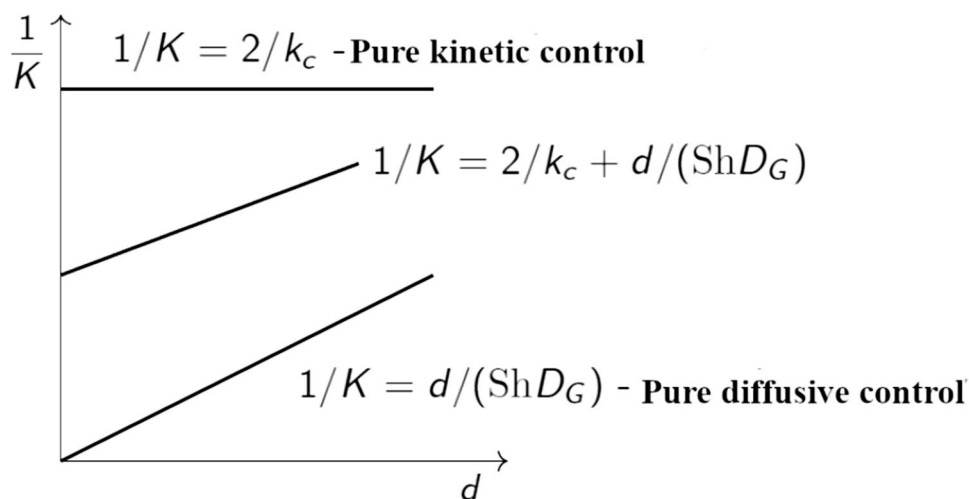
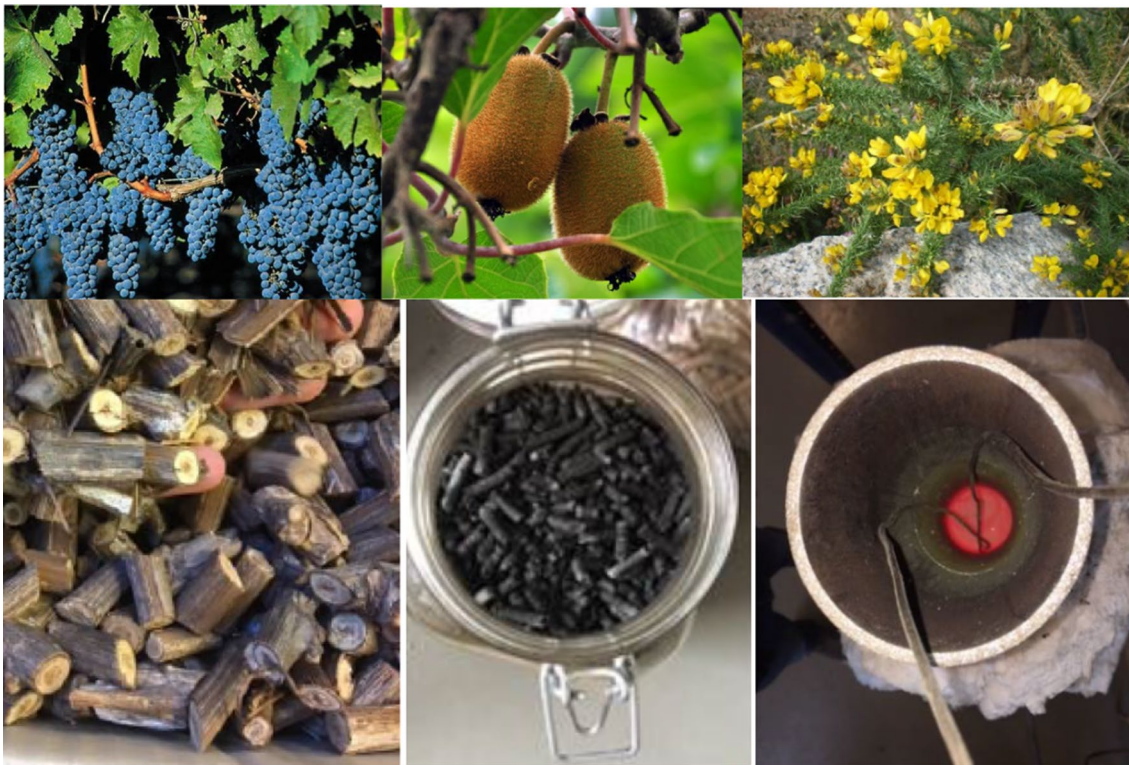
Pedro Resende
pedroresende@estg.ipv.pt

¹ INEGI, Campus da FEUP, Rua Dr. Roberto Frias, 400, Porto 4200-465, Portugal

² ProMetheus, ESTG, Instituto Politécnico de Viana do Castelo, Viana do Castelo 4900-347, Portugal

³ CEFT-DEMEC, Universidade do Porto, Rua Dr. Roberto Frias, s/n, Porto 4200-465, Portugal

Graphic Abstract



Keywords Biochar · Bubbling fluidized bed · Combustion · Diffusion · Kinetics

List of symbols

Greek Symbols

$\Delta h'$	Enthalpy of combustion for the carbon to CO oxidation [kJ/kg]
ϕ_p	Sphericity of a char particle [-]
σ	Stefan–Boltzman constant [W/(m ² K ⁴)]
ε_p	Emissivity of a char particle [-]

Roman Symbols

A	Pre-exponential factor [m/s]
A_p	Surface area of a char particle [m ²]
A_s	Surface area of a sphere with the same volume [m ²]
c_{pg}	Constant pressure specific heat of gas [J/(kg K)]
C_p	Molar concentration of oxygen in the particulate phase [kmol/m ³]

C_s	Molar concentration of oxygen at the particle surface [kmol/m ³]
d	Corrected spherical diameter of the particle [m]
d_s	Diameter of a sphere with the same volume [m]
D	Diameter of a cylindrical particle [m]
D_G	Oxygen diffusivity in the air [m ² /s]
E_a	Activation energy [J/mol]
f_c	Mass fraction of carbon [–]
f_{cf}	Mass fraction of the fixed carbon [–]
f_{cv}	Carbon mass fraction in the volatiles [–]
f_v	Volatiles mass fraction in the char particles [–]
h_{O_2}	Oxygen enthalpy [kJ/kg]
h_C	Carbon enthalpy [kJ/kg]
h_{CO}	Carbon monoxide enthalpy [kJ/kg]
k_c	Reaction rate constant for the heterogeneous reaction [m/s]
k_{tg}	Gas thermal conductivity [W/(m K)]
K	Overall combustion resistance [s/m]
L	Length of a cylindrical particle [m]
\dot{m}_{O_2}	Oxygen mass flow rate [kg/s]
\dot{m}_C	Carbon mass flow rate [kg/s]
\dot{m}_{cf}^i	Mass of carbon consumed until time instant i [kg]
\dot{m}_{CO}	Carbon monoxide mass flow rate [kg/s]
M_C	Molecular mass of carbon [kg/kmol]
$M_{C_3H_8}$	Molecular mass of propane [kg/kmol]
\bar{n}	Generic molar concentration [kmol/m ³]
\dot{N}_{O_2}	Molar oxygen flow rate reaching the particle surface [kmol/s]
\dot{Q}_{s-g}	Heat transfer rate towards the gas around the particle [W]
\dot{Q}_{s-i}	Heat transfer rate towards the center of the particle [W]
\dot{Q}_{rad}	Heat transfer rate through radiation [W]
\underline{R}_0	Carbon molar consumption rate [kmol/s]
\bar{R}	Universal gas constant [J/(kmol K)]
Sh	Particle Sherwood number [–]
t^i	Time instant i [s]
T	Temperature [K]
T_b	Bed temperature [K]
T_p	Particle temperature [K]
U	Fluidization velocity [m/s]
U_{mf}	Minimum fluidization velocity [m/s]
\dot{V}_{air}	Volume flow rate of air [m ³ /s]
$x_{CO_2}^i$	Carbon dioxide molar fraction at time i [–]

Statement of Novelty

The present study is about the determination of kinetic and diffusive data from the bubbling fluidized bed combustion of chars made from pellets fabricated with pruning wastes of vine (*Vitis vinifera*) and kiwi (*Actinidia deliciosa*) plants, and gorse (*Ulex europaeus*) forestry residues. These

biomass wastes were collected in the Galicia-Northern Portugal Euroregion. In this Euroregion there is a huge energy potential in agricultural and forestry wastes to be exploited and this work is a part of a wider study to evaluate such potential. It is an extension of a previous work presented at ICEER2019 [1], expanding the range of information in the study. Now it takes into account the importance of the combustion of the volatiles of the biochars on the total carbon balance, as well as the non-sphericity of the fuel particles, parameters discarded in the first study. The first paper had also no information on the combustion of gorse char particles. This new detailed information of the combustion data related to the above-mentioned biochars, leads to a more reliable set of results.

Introduction

The biomass was always one of the greatest sources of primary energy of the different human societies [2] and its importance is rising again because of the pollution issues and subsequent climatic changes, as it is considered almost a carbon dioxide neutral renewable energy source [3]. Its properties are greatly dependent upon the fuel being used and the required pre-processing [4], such as the pelletization, which is one of such pre-processing steps that is typically adopted for the energy densification of biomass [5].

The agricultural and forestry residues have been considered as an accessible and affordable source of biomass energy [6]. There is however a lack of information concerning the combustion kinetic data of many agricultural and forestry residues especially in the Galicia-Northern Portugal Euroregion, where waste values of 2 to 5 t/ha/year are common. In the present study on the fluidized bed combustion of chars made from pruning wastes of vine (*Vitis vinifera*) and kiwi (*Actinidia deliciosa*) plants and gorse (*Ulex europaeus*) forestry residues, diffusive and kinetic data were determined. These data are fundamental for the design, construction and adequate operation of industrial burning equipment.

The bubbling fluidized bed reactor is a good tool to determine diffusive and kinetic data for the combustion of different biomasses. It allows high heat and mass transfer rates, guarantees good temperature uniformity in the reacting region and it is indicated for the combustion of high ash content solid fuels [7, 8]. The woody biomass from Portuguese origin has been the subject of several studies. Fluidized bed combustion results of commercial and recarbonized chars of nut pine (*Pinus pinea*) and cork oak (*Quercus suber*) were discussed [9, 10], as well as the influence of the fragmentation phenomenon upon the determination of kinetic and diffusive data on the fluidized bed combustion of nut pine chars [11]. Tomé et al. [12] studied the fluidized bed combustion of chars made

from biomass of Mozambican origin. This type of study was extended to Brazilian biomass, where biochars from eight species of wood obtained from the semiarid region of the Brazilian northeast known as the Cariri Paraibano, were also analyzed [13]. Following the same procedure, biochars obtained from woody biomasses from the central region of Portugal, holm oak (*Quercus ilex*), eucalyptus (*Eucalyptus globulus*), maritime pine (*Pinus pinaster*), and cork oak (*Quercus suber*), were also studied [14], and the importance of particle sphericity and fragmentation on the behavior of these four chars was discussed [15].

More recently, interest turned to the study of combustion of pellets made from invasive shrubs and trees, which although being considered harmful vegetable species, should in fact be considered valuable biomass energy resources [16–19]. The influence of mineral ash components in the char ashes upon the kinetic behavior during combustion was also an object of study [20, 21]. The interest of using crop and forest residues as energy sources, although going back several years, has only been more recently the target of much more scientifically orientated studies [22], although the ash-related issues have always been a subject of deep concern during biomass combustion [23].

The tested chars in the present study were made from pellets fabricated with the three mentioned biomasses. The pellets were carbonized at 900 °C (kiwi and vine) and 800 °C (gorse), in a bed fluidized by nitrogen. During solid biomass combustion, after the initial particle heating and drying phase there is the subsequent combustion of the released volatile matter, with formation of a carbonaceous solid core. The combustion of this core is the last and longer step of the solid biomass combustion process [4]. As solid fuels can be burned at temperatures up to 1000 °C, depending on the type of burner used [23], this explains the choice of the above carbonization temperatures for the production of the biochars to be tested. The objective of the experiments was thus to find out the mechanisms controlling the combustion process of such chars to optimize the operating conditions of the industrial burning equipment when using this type of agricultural waste.

Materials and Methods

The kiwi and vine biomasses from agricultural plant pruning and the gorse from forest cleaning processes, were collected in the Galicia-Northern Portugal Euroregion. Subsequently pellets were fabricated at the Viseu Polytechnic Institute in Portugal and were then carbonized at INEGI in a bubbling fluidized bed reactor. The pellets were placed inside a stainless steel mesh bag and immersed in the bed fluidized by nitrogen, to prepare the char particles. After the carbonization step, the stainless steel bag was extracted from the fluidized bed and cooled in nitrogen. Subsequently, the char particles were manually separated into five different sizes. Table 1 shows the results of the biochars proximate analysis, as well as the corresponding densities obtained through the mercury pycnometry technique.

The laboratory scale fluidized bubbling bed that was initially used as a carbonizing and subsequently as a combustion reactor, was built with a refractory steel tube with an internal diameter of 80 mm and 1500 mm length. The bed was formed by silica sand particles with an average diameter of 283 µm and 200 mm height., supported by a stainless steel distributor containing 101 orifices with 0.3 mm diameter. In Fig. 1 there is an overall scheme of the experimental setup.

The bed is externally heated by an electrical resistance of 4 kW, controlled by a PID controller. Two K type thermocouples (ST1 and ST2) measure the bed temperature. The ST1 is connected to the PID controller of the bed heating electrical resistance, while the readings from ST2 are sent to a data acquisition board PD2, installed in a desktop computer. A stainless steel suction probe, located above the bed free surface, collects samples of exhaust combustion gases.

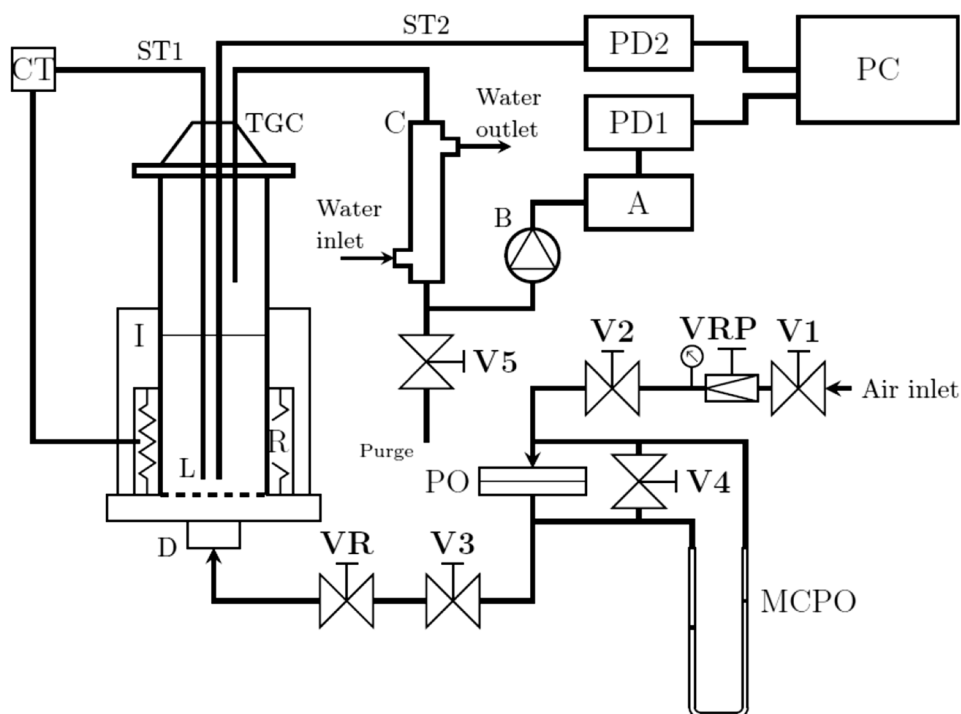
The sampled flow of combustion gases is sent to a condenser and then to a volumetric sampling pump, and afterwards the cooled dry gas flow is directed to a CO₂ gas analyzer. The infrared CO₂ analyzer (Signal, model 7000FM GFC) is connected to a data acquisition system from Measurement Computing. This data acquisition system is composed by two independent boards, PCI-DAS-TC (PD2) and PCI-DAS16JR/16 (PD1), receiving signals from the thermocouples and the gas analyzer, respectively. The registration of the collected data was managed by the DasyLab software

Table 1 Proximate analysis of kiwi, vine and gorse chars

Parameter	Analytical method	Kiwi	Vine	Gorse
Moisture at 105 °C	CEN-14774-1	3.5	3.7	1.5
Volatile matter at 900 °C (%) D. B	CEN-15148	14.0	16.6	4.3
Ashes at 550 °C (%) D. B	CEN-14775	14.3	12.0	10.9
Fixed carbon (%) D. B	Calculated	71.7	71.4	84.8
Density [kg m ⁻³]		820.7	798.7	829.2

D.B. dry basis

Fig. 1 Scheme of the experimental setup



and data treatment was carried out by means of the Spyder software, a Python scientific environment [24].

For each experimental test, the char particles were selected and classified according to their sizes. The extremities of the char particles were cut to give them a cylindrical morphology, with diameters ranging from 5 to 6 mm, for kiwi and vine char particles, and from 4 to 5 mm for the gorse char particles. The corresponding lengths allowed the definition of several classes of particle classification, as specified in Table 2, five for kiwi and vine chars and four for gorse chars.

The combustion tests were carried out for each size class characterized by the corresponding length to diameter ratio (L/D) using 2 g batches measured in a Sartorius MA 30 balance. The mass and number of particles of each test batch were registered for further analysis.

Figure 2 shows the sequence procedure of the experiments: the particle sanding and storage, the batch preparation and finally the beginning of a combustion experiment

with the introduction of the char particles in the bubbling fluidized bed reactor.

The combustion experiments were carried out at bed temperatures of 750, 820, 850 and 900 °C. To follow up the development of the batch combustion process the CO_2 molar concentration in the flow of exhaust gases was continuously measured and registered, as well as the bed temperature, both at a rate of 1 Hz. A detailed analysis was performed with 49 experiments using a superficial velocity ratio of $U/U_{mf} = 2$, for all tests. The U_{mf} values were experimentally determined: 44.0 mm/s at 750 °C; 42.1 mm/s at 820 °C; 41.4 mm/s at 850 °C; and 40.2 mm/s at 900 °C. This velocity ratio was enough for the purpose of the studies and had the advantage of minimizing the elutriation of small particles resulting from the attrition and fragmentation of the fuel particles. With this fluidizing velocity, the carbon losses from the bed was minimized, improving the overall carbon balance required for the calculation of the time evolution of fuel particle dimensions along the combustion process. Table 3 shows the mass and

Table 2 Size classes of char particles

L/D	Kiwi		Vine		Gorse	
	L_{min}	L_{max}	L_{min}	L_{max}	L_{min}	L_{max}
1	5	6	5	6	–	–
1.5	8	9	8	9	6	7
2	11	12	11	12	9	10
3	15	16	15	16	13	14
4	21	22	21	22	18	19

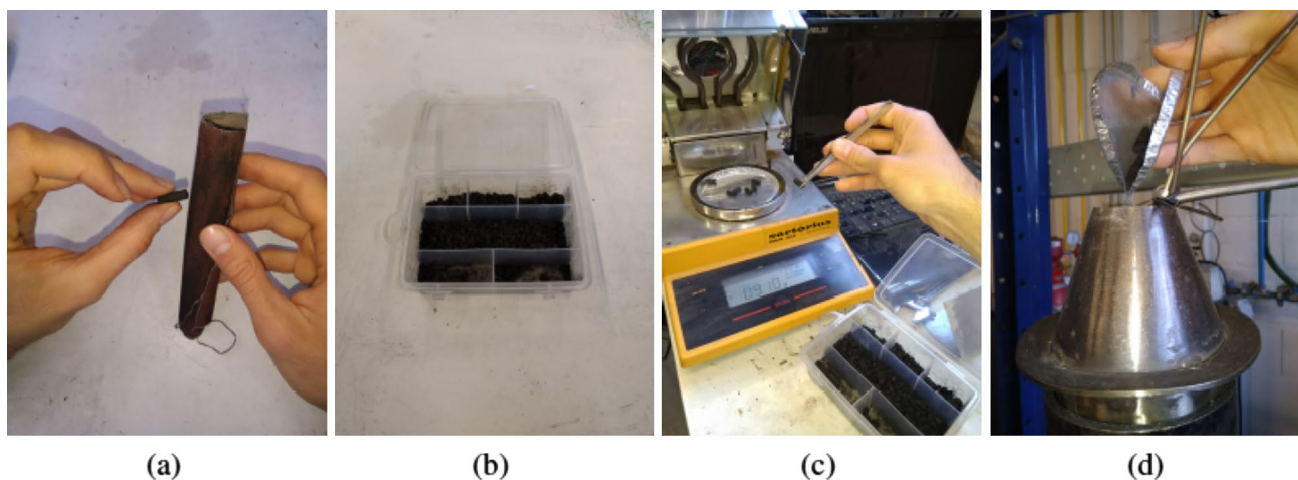


Fig. 2 **a** Particle sanding process; **b** particle storage; **c** batch weighing and **d** batch introduction in the bubbling bed

the particle number for each tested batch, as well as the corresponding bed temperature.

The average uncertainties of the experiments were of 0.179% (v/v) for the CO₂ measurement, 0.76% for the fluidized bed temperature and in the range of 8.6 to 16.6% for the mass flow rate of the fluidization air. These values include the whole measurement chain, i.e., up to the computer output.

Results and Discussion

Evolution of the CO₂ in the Exhaust Gas Flow

Figure 3 presents typical evolutions of the molar concentration of CO₂ in the exhaust gas flow for combustion experiments with kiwi char. The curve trends are quite similar for all tested bed temperatures. In the first instants, after the introduction of the batch of char particles, there is a peak on

Table 3 Characterization of the tested biochar batches

T [°C]	Kiwi		Vine		Gorse		
	L/D	m_b [g]	N_p	m_b [g]	N_p	m_b [g]	N_p
750	1	2.045	33	2.032	33		
	1.5	2.021	16	2.045	20	2.024	31
	2	1.987	23	7.997	14	1.996	19
	3	1.911	11	2.078	11	2.076	14
	4				2.009	8	2.076
820	1	2.001	32	1.999	32		
	1.5			1.983	19	1.982	31
	2	1.969	15	1.984	14	2.012	20
	3	2.070	12	1.984	10	1.973	13
	4					2.078	10
850	1	2.009	34	1.980	31		
	1.5	2.009	21	2.038	20	2.004	29
	2	2.055	16	2.105	15	2.046	19
	3	2.003	12	2.005	11	2.061	13
	4					1.939	9
900	1	2.001	33	2.030	33		
	1.5	2.023	21	2.024	21	2.029	30
	2	1.970	15	2.005	14	2.002	19
	3	1.968	11	2.034	11	2.087	14
	4					1.949	9

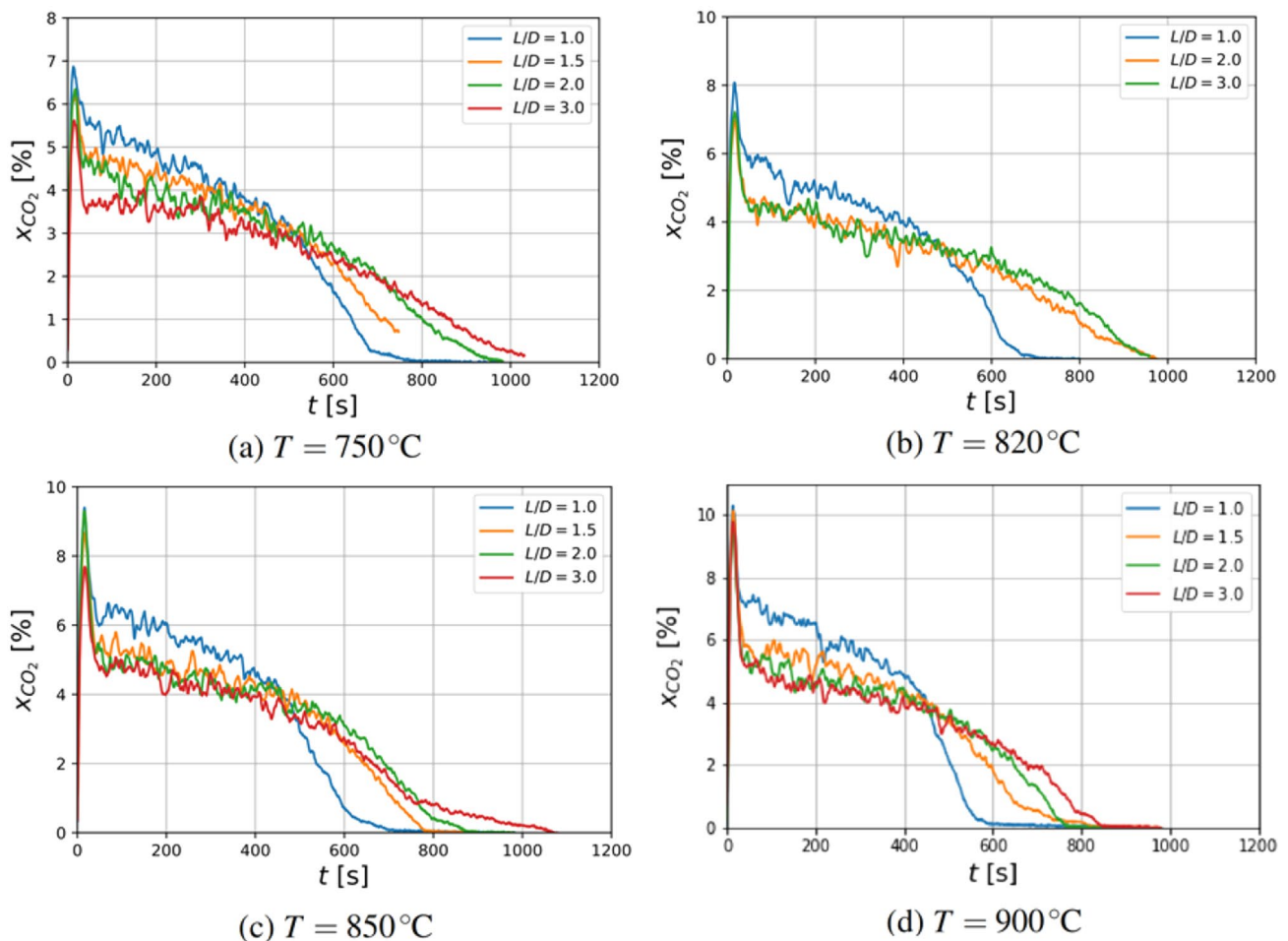


Fig. 3 CO₂ time evolution in the exhaust combustion gases for kiwi char particles

the CO₂ release rate followed by a continuous concentration declining. Initially, in this declining region, the reduction of concentration is quite smooth, followed by a stronger concentration reduction, being this reduction stronger for lower L/D ratios.

Riaza et al. [25] analyzed images of the combustion of individual particles and registered that the first step of the combustion process is the particle heating with consequent drying and release of volatiles, and only after this initial step the combustion of the solid residues takes place. Van Loo and Koppejan [4] and Wang et al. [26], from the study of thermogravimetric (TG) curves and differential thermogravimetric (DTG) curves confirm that the combustion of solid residue only takes place after volatiles release. Volatiles are mainly composed by light hydrocarbons, carbon monoxide and dioxide. Neves et al. [27] analyzed the volatile gas composition during the fluidized bed pyrolysis of two ligneous biomasses and realized that the majority of the volatiles were released around 600 °C, although some components like ethylene, C₂H₄, methane, CH₄, and carbon monoxide, CO,

reach their peak about 900 °C. In the preparation of the chars used in the present study the wood pellets pyrolysis was done at 900 °C, while the gorse was carbonized at 800 °C, and for calculation purposes it is assumed that the volatiles that might be released in their combustion is propane, C₃H₈. Not knowing the composition of the remaining volatiles that are being released during the combustion of the char particles, it is necessary a careful approach in order to carry out an adequate carbon balance. Hesketh and Davidson [28] and Ribeiro and Pinho [29] used propane to simulate the volatiles released from burning coke particles. Following such approach, in this work the volatiles released during the bio-char particles combustion were assumed as propane. With this methodology, the carbon balance of the combustion process, obtained through the time integration of the CO₂ concentration in the exhaust gases, is accomplished, and a carbon recuperation close to 100% is achieved. It should be emphasized that kiwi, grapevine and gorse chars contain 14.0% (m/m), 16.6% (m/m) and 4.3% (m/m) of volatiles, respectively, as can be observed in Table 1.

In this situation, the mass fraction of carbon f_c , in a given sample of biochar to be burned, is the summation of the fixed carbon and the carbon in the volatiles

$$f_c = f_{cf} + f_{cv} \quad (1)$$

where f_{cf} is the mass fraction of the fixed carbon and f_{cv} is the carbon mass fraction in the volatiles determined by means of

$$f_{cv} = \frac{3 M_C}{M_{C_3H_8}} f_v \quad (2)$$

In Eq. 2 M_C and $M_{C_3H_8}$ are respectively the molecular masses of carbon and propane and f_v is the volatiles mass fraction in the char particles. From the calculation the following values are determined, $f_{cv} = 11.45\%$ and $f_c = 83.20\%$.

Figure 4 shows the CO_2 released evolution during an experiment for kiwi char particles with a L/D ratio of 1 and a bed temperature of $750^\circ C$, and as can be observed it is possible to identify two stages: the first stage (red line) represents the time evolution of the CO_2 formed during the propane (volatiles) combustion, as the release of volatiles occurs at the beginning of the combustion process, of a given batch of coal particles; and the second stage (blue line) which refers to the CO_2 released through the combustion of the carbonaceous solid residue. As observed the initial CO_2 release peak stays inside the initial red zone (Fig. 4).

During the second stage, the combustion of the solid carbonaceous residue, the smaller the particles, the faster is the combustion reaction because of the higher surface area available for the heterogeneous phase reaction of carbon oxidation to carbon monoxide. There is so a higher reaction rate as detected by the stronger slope in the curves shown in Fig. 3. At the end of the solid residue combustion, the reaction rate increases due to the particle fragmentation [11, 15, 30], which increases the superficial reaction area, leading

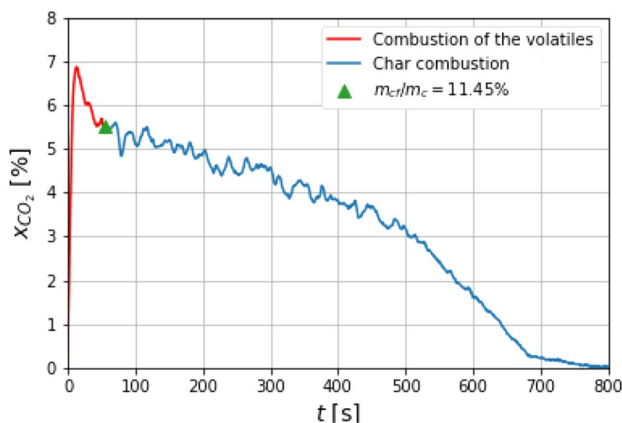


Fig. 4 CO_2 time evolution in the exhaust combustion gases for kiwi char particles $L/D = 1$ and a bed temperature of $750^\circ C$

to a stronger decaying of the CO_2 curve. It is also clear that the higher the bed temperature the stronger is the CO_2 decay meaning that the value of the kinetic and diffusive resistances are becoming smaller (Figs. 3, 5 and 6).

The combustion behavior of the vine char is similar to the kiwi char. Figure 7 shows equally time evolutions of the CO_2 concentration in the combustion exhaust gases for different L/D ratios and four bed temperatures, namely 750 , 820 , 850 and $900^\circ C$. The same initial peak of the CO_2 curve, and again the same CO_2 evolution corresponding to the combustion of the carbonaceous solid residue. For the same assumption of considering that propane is representative of the released volatiles, the following results are obtained for vine char particles, $f_{cv} = 13.60\%$ and $f_c = 85.00\%$.

The gorse char has a lower volatiles percentage, 4.3% (w/w), leading to a different time evolution of CO_2 in the first stage and, as expected, the peak magnitude decreases when compared to the others biochars previously presented, Fig. 6. However, concerning to the combustion of the solid carbonaceous residue, its behavior is similar to the previously biochars, the kiwi and the vine char. The carbon content in the volatiles and in the carbonaceous residues are respectively $f_{cv} = 3.5\%$ and $f_c = 88.3\%$.

Overall Resistance to Combustion

From the integration of the CO_2 versus time curve, and knowing the number of particles composing a batch under combustion, it is possible to determine for each time instant the burned mass fraction of carbon, the particle size and the instantaneous reaction rate and finally the time evolution of the overall resistance to combustion [9–11]. To determine the carbon burned m_{cf} up to a given time instant, the CO_2 versus time curve is integrated according to Eq. 3 of the trapezium rule,

$$m_{cf}^i = M_C \dot{V}_{air} \bar{n} \frac{x_{CO_2}^i + x_{CO_2}^{i-1}}{2} (t^i - t^{i-1}) + m_{cf}^{i-1} \quad (3)$$

where i represents the present time instant while $i-1$ represents the former time instant, \bar{n} is the generic molecular concentration in the exhaust gas flow, t is a generic time instant and \dot{V}_{air} is the volume flow rate of air, assumed equal to the flow rate of the combustion products.

The evolution of the overall combustion resistance, as a function of the mean diameter of the particles, is calculated using mathematical models developed for the fluidized bed combustion of char particles, assuming that they are spherical. However, this hypothesis normally does not occur and accordingly the combustion data must be analyzed taking the particle non-sphericity into account. In the present study cylindrical particles with different length to diameter ratios L/D , were considered. The sphericity of the particles must

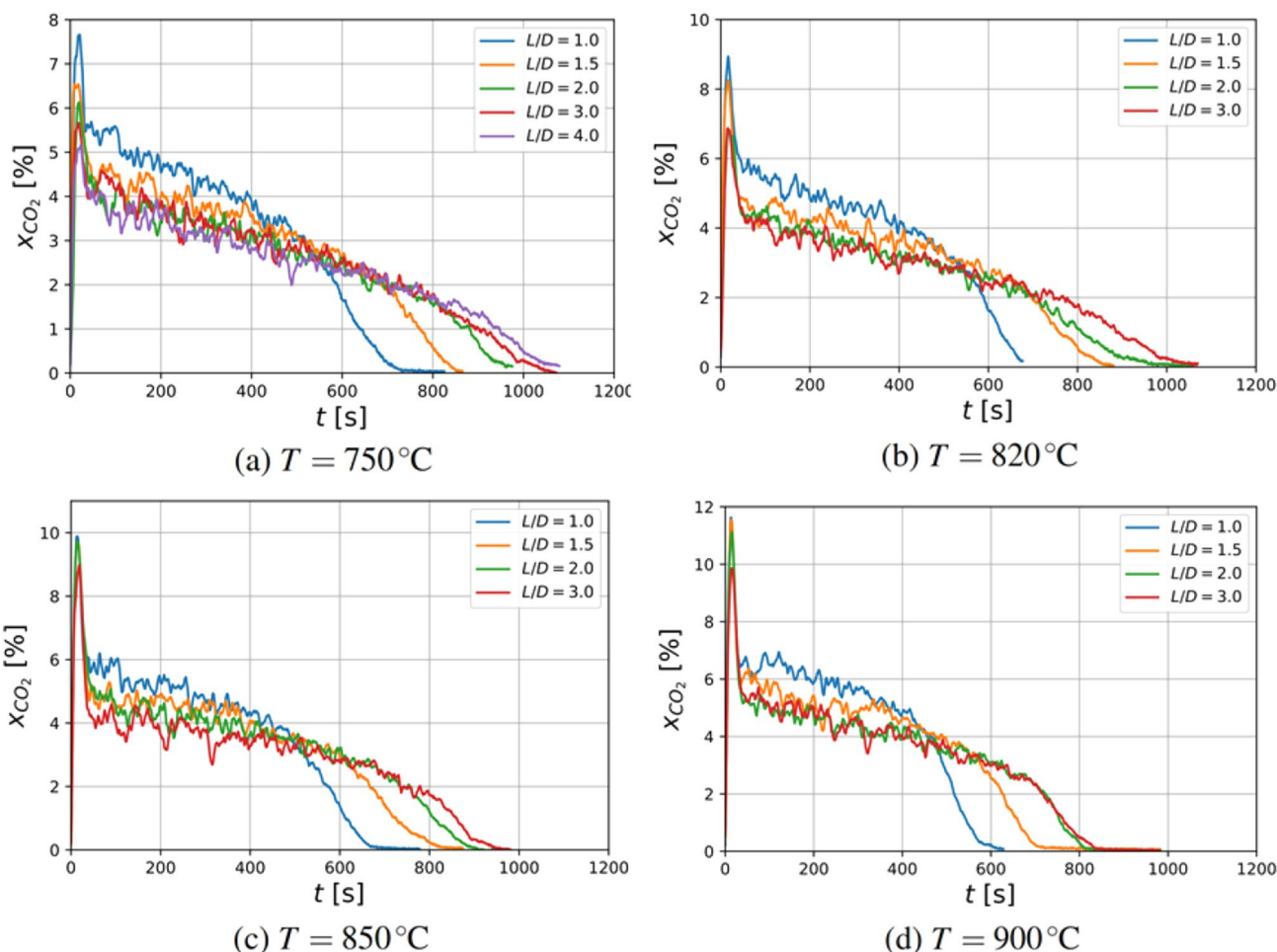


Fig. 5 CO₂ time evolution in the exhaust combustion gases for vine char particles

then be taken into consideration, in order to reach a better characterization of the volume and surface area of the particles composing a given batch of char particles.

The corrected spherical diameter of the particle is the product of the diameter of a sphere with the same volume as the particle d_s with the particle sphericity [15],

$$d = \phi_p d_s \tag{4}$$

being ϕ_p , the particle sphericity, given by,

$$\phi_p = \frac{A_s}{A_p} \tag{5}$$

and taking into account the real L/D ratio of the particle,

$$\phi_p = \left(\frac{3}{2}\right) \frac{(L/D)^{2/3}}{(L/D) + 1} \tag{6}$$

In Table 4 are the corresponding sphericities for all the particles tested.

This type of approach has already been used in several experimental studies [15, 31]. The correct use of the particle sphericity leads to a precise understanding of the combustion control mechanisms. Figure 9 presents the overall combustion resistance as a function of the particle diameter for combustion experiments of vine char at 850 °C, with and without the sphericity correction. If, for a given situation, the influence of the particle non-sphericity is not accounted for, a wrong interpretation of the results might occur. In Fig. 7, it is possible to observe the influence of the L/D ratio on the control of the combustion process. The left side plots, Fig. 7a and c, were obtained by non-applying the sphericity correction leading to the erroneous idea of a purely kinetically controlled combustion process. The right side plots, Fig. 7b and d, were obtained using the non-sphericity correction, leading to a correct interpretation of the relative influence of diffusion and kinetics upon the combustion control.

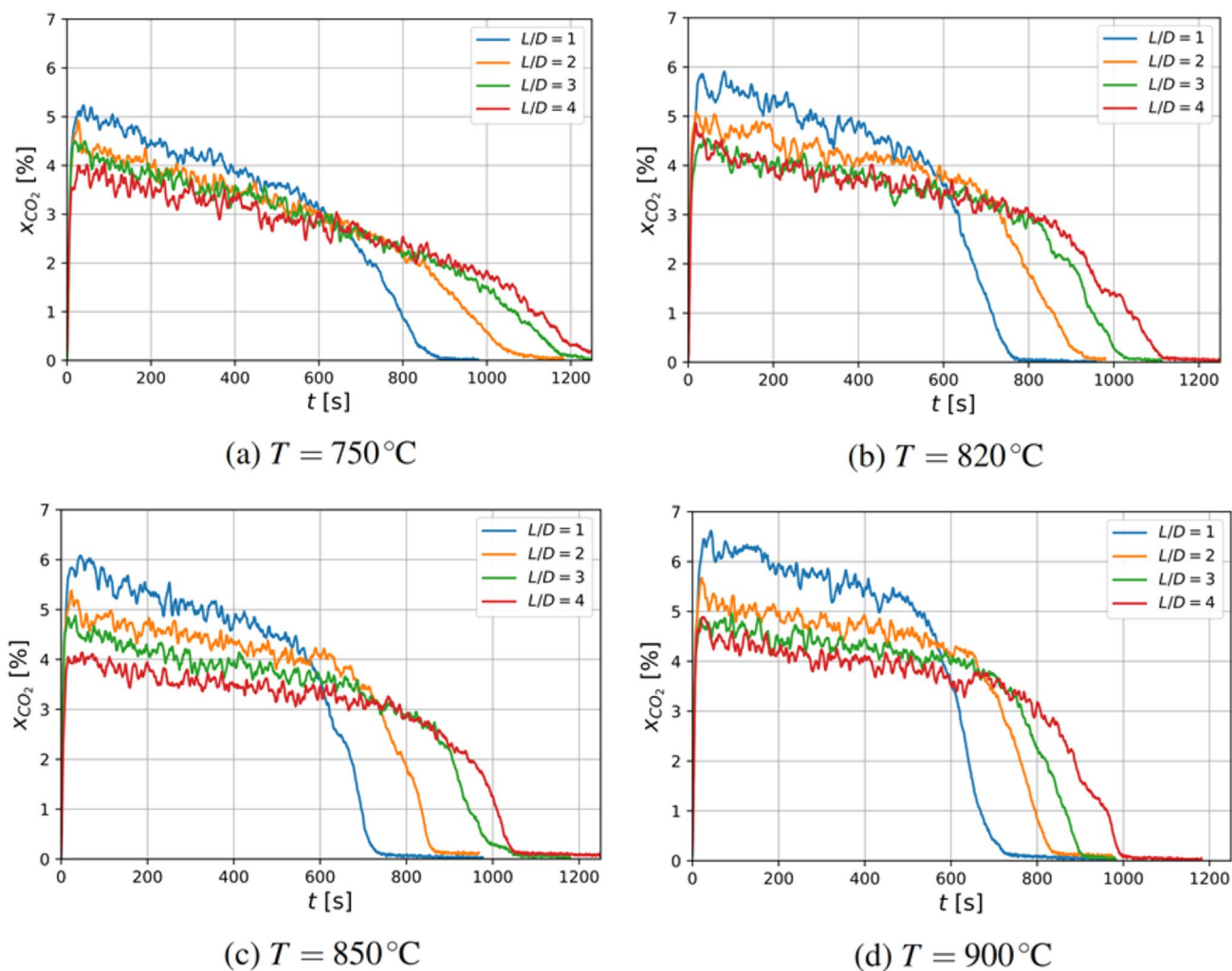


Fig. 6 CO₂ time evolution in the exhaust combustion gases for gorse char particles

Kinetic and Diffusive Results

To determine the kinetic and diffusive information from the evolution of the overall combustion resistance, the transient initial and final regions of this evolution were discarded and only data in the 30 to 70% burned mass fraction were considered. Accordingly, the next plots, Figs. 8, 9 and 10 show the $1/K$ versus corrected d for the kiwi, vine and gorse char pellets respectively. Only 10% of the experimental points are

presented in the plots, to keep them readable. However, the calculations were carried out with all the available experimental points.

In the batch combustion experiments carried out in the fluidized bed, the solid particles are assumed spherical and burn at a constant density, n_m and reducing size. It was also considered that the particle carbon burns to CO according to $C + \frac{1}{2} O_2 \rightarrow CO$ and the CO formed burns away from the particle according to $CO + \frac{1}{2} O_2 \rightarrow CO_2$ [32], which is a further evolution from the initial model established by Avedesian and Davidson [33]. Thus, the oxygen consumption rate at the surface of the particle is then half the carbon consumption rate and the heterogeneous phase reaction that takes place at the particle surface is a first order reaction,

$$\dot{N}_{O_2} = \frac{1}{2} R_0 = \pi d Sh D_G (C_p - C_s) = \frac{1}{2} k_c \pi d^2 C_s \quad (7)$$

Table 4 Sphericities of the char particles as a function of the corresponding L/D ratios

L/D	ϕ_p
1	0.8736
1.5	0.8585
2	0.8320
3	0.7788
4	0.7338

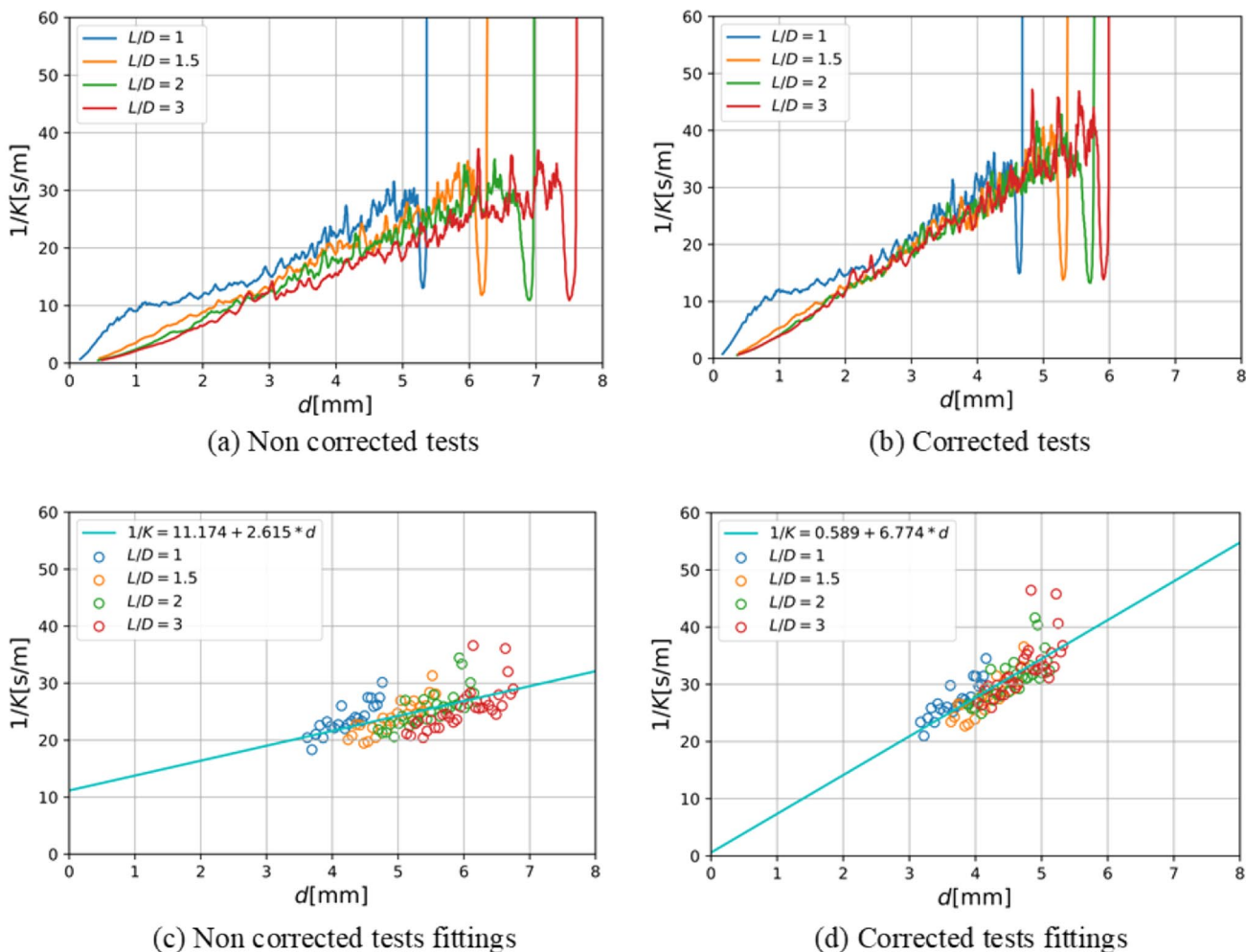


Fig. 7 Influence of the sphericity correction on the evaluation of the overall combustion resistance

where \dot{N}_{O_2} is the molar oxygen flow rate reaching the particle surface, R_0 is the carbon molar consumption rate, Sh is the particle Sherwood number, d is the diameter of the burning particle, D_G is the oxygen diffusivity in the air, C_p and C_s are respectively the molar concentrations of oxygen in the particulate phase of the bed and at the surface of the burning particle. k_c is the reaction rate constant for the heterogeneous phase reaction occurring at the surface of the char particle. Manipulating the above equation, it is possible to write that,

$$R_0 = 2 \pi K d^2 C_p \tag{8}$$

wherein, $1/K$ is the overall combustion resistance [10, 11] for the combustion of batches of carbon particles in a bubbling fluidized bed combustor. As can be seen from Eq. 9, after a mathematical manipulation of the Eq. (8) [10, 11], the first term of the second member is the particle external diffusion resistance, while the second term concerns the heterogeneous phase carbon-to-carbon monoxide reaction resistance.

$$\frac{1}{K} = \frac{d}{Sh D_G} + \frac{2}{k_c} \tag{9}$$

It is understandable that from the slope of the $1/K$ versus d diffusive information can be gathered through the Sherwood number, while from the intercept the heterogeneous reaction rate constant k_c is determined. Table 5 presents the determined kinetic and diffusive data.

From the analysis of the results available in Table 5, it can be concluded that the reaction control is shared by the diffusion and the heterogeneous phase reaction kinetics, for the kiwi and vine chars, while for the gorse char above 850 °C the combustion control is purely diffusive. The values of the Sherwood number are similar to those found in other studies of the same group covering Brazilian, Mozambican and Portuguese biochars [10, 12–14].

To get adequate information from the kinetic data it must be taken into account that

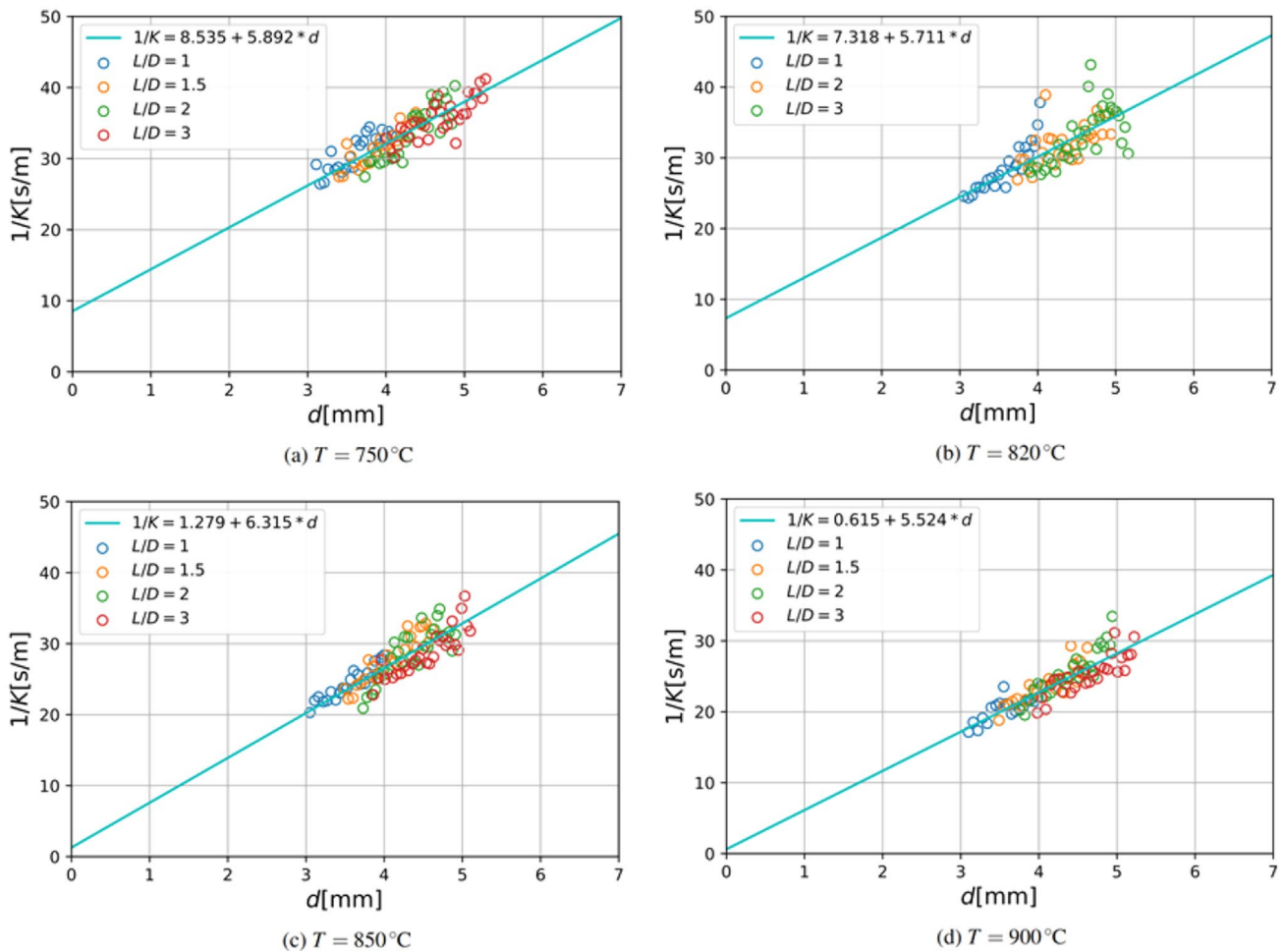


Fig. 8 Straight-line fitting for the kiwi char overall combustion resistance

$$k_c = A \exp \left(-E_a / (\bar{R} T_p) \right) \tag{10}$$

where \bar{R} is the universal gas constant and T_p the particle temperature, A the pre-exponential factor and E_a the activation energy. From a logarithmic plot of $\ln k_c$ versus $1/T_p$,

$$\ln k_c = \ln A - E_a / (\bar{R} T_p) \tag{11}$$

a linear trend line can be theoretically obtained and, from its slope and interception, information on the activation energy and on the pre-exponential factor is obtained. However, to get the right information from the kinetic results it is necessary to know the burning particle temperature, which is normally above the fluidized bed temperature. However, the measurement of the wandering particles temperature is impossible. The option adopted in this work, as in many other previous works of the group [13, 14, 34], is to carry

out an energy balance of the particle and from it obtain the corresponding particle temperature. The scheme of the energy balance of a carbonaceous particle is in Fig. 11.

Figure 11 shows the energy transfer, taking place at the surface of a burning carbon particle. Assuming that for short time intervals there is no heat transferred towards the particle interior, and taking into account that the process can be considered a steady state one, the energy balance is simplified to:

$$\dot{m}_C h_C + \dot{m}_{O_2} h_{O_2} - \dot{m}_{CO} h_{CO} = \dot{m}_c \Delta h' \tag{12}$$

where, $\dot{m}_C h_C$ is the energy of the carbon; $\dot{m}_{O_2} h_{O_2}$ is the energy of the oxygen flow; $\dot{m}_{CO} h_{CO}$ is the energy of the carbon monoxide flow and $\Delta h'$ is the heat of combustion of $C + 1/2O_2 \rightarrow CO$ at the bed temperature. The result is then [34],

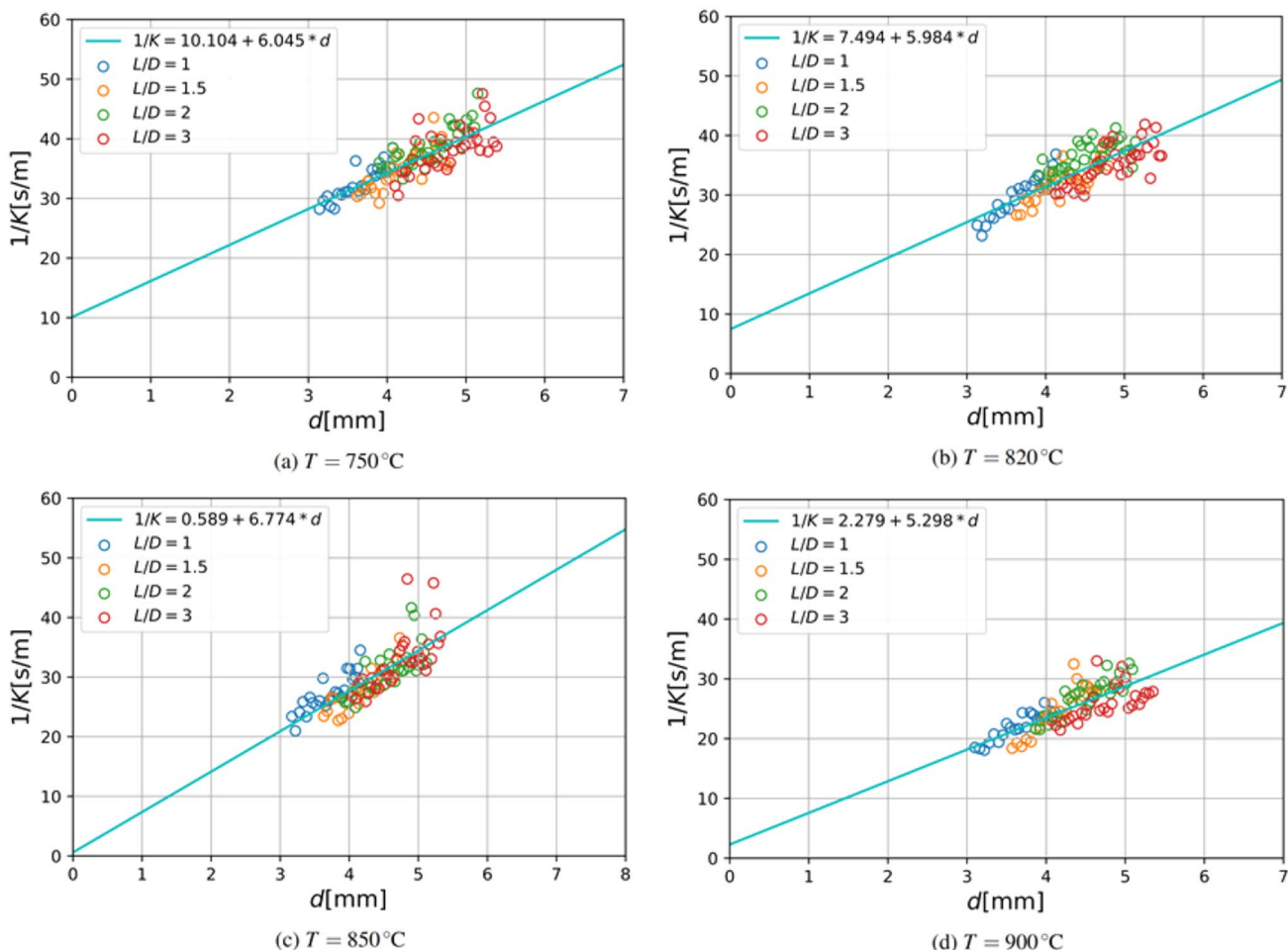


Fig. 9 Straight-line fitting for the vine char overall combustion resistance

$$\dot{m}_C \Delta h' + \dot{m}_C c_{pg} (T_p - T_b) \frac{\exp\left(-\frac{\dot{m}_C c_{pg}}{2 \pi d k_{ig}}\right)}{1 - \exp\left(-\frac{\dot{m}_C c_{pg}}{2 \pi d k_{ig}}\right)} + \epsilon_p \pi d^2 \sigma (T_p^4 - T_b^4) = 0 \tag{13}$$

where, $\Delta h' = 9211\text{kJ/kg}$ at 25°C , ignoring its temperature dependence. T_p is the particle temperature, T_b is the bed temperature, $\epsilon_p = 0.95$ is the emissivity of a carbon particle, σ is the Stefan–Boltzman constant, k_{ig} is the thermal conductivity of the gas evolving the burning carbon particle, which was assumed equal to the thermal conductivity of the air at bed temperature. c_{pg} is the specific heat of the gas evolving the burning carbon particle; d is the diameter of the burning carbon, and \dot{m}_C is the burning rate of the carbon particle, given by [34],

$$\dot{m}_C = 2 M_C \pi d^2 K C_p \tag{14}$$

being C_p the average molar O_2 concentration inside the bed dense phase, and $1/K$ the overall fluidized bed combustion resistance.

By means of Eq. 13 the instantaneous particle temperatures were determined for each experiment. Table 6 presents the average particle temperature for each bed temperature and biomass species through a program routine as well as the corresponding reaction rate constants and the average temperature difference between the bed and the burning particle temperature.

Figures 12 and 13 present the plot of $\ln k_c$ versus $1/T$ and the corresponding fitting straight lines for kiwi and vine chars. As above a bed temperature of 820°C , the gorse char

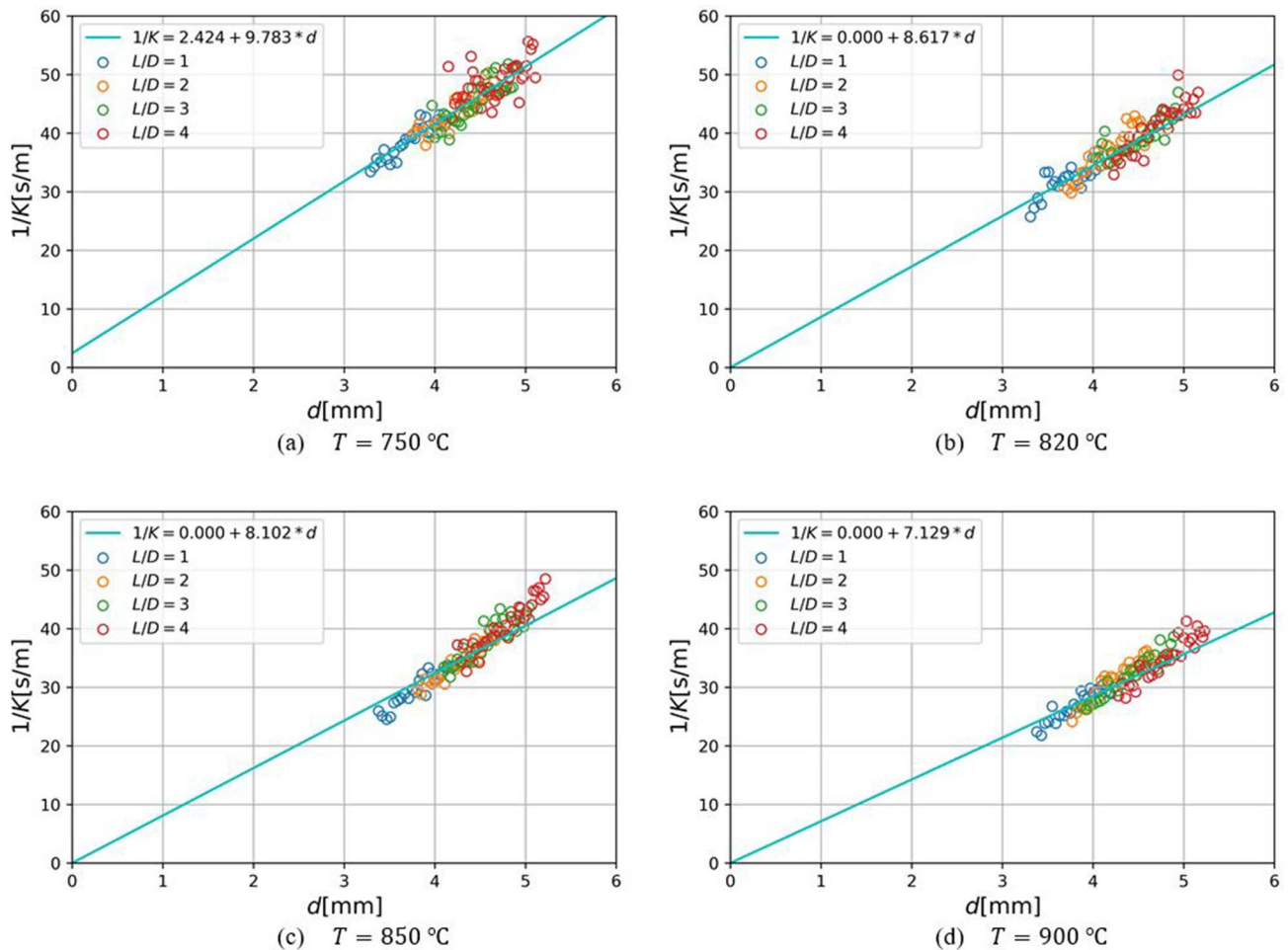


Fig. 10 Straight-line fitting for the gorse char overall combustion resistance

Table 5 Kinetic and diffusive results for the three tested chars

T [°C]	Kiwi		Vine		Gorse	
	Sh	k_c [ms ⁻¹]	Sh	k_c [ms ⁻¹]	Sh	k_c [ms ⁻¹]
750	1.2704	0.2343	1.2383	0.1979	0.7813	0.6096
820	1.1868	0.2733	1.1326	0.2669	0.7866	∞
850	1.0306	1.5639	0.9607	3.3955	0.8032	∞
900	1.1036	3.2500	1.1507	0.8774	0.8552	∞

combustion has a pure diffusive control, no kinetic data can be obtained for this last char.

Table 7 shows the activation energy and the pre-exponential factor for the kiwi and vine chars, determined from the Arrhenius straight-line fitting.

The activation energies are comparable with those from other authors. Rangel and Pinho [10] present activation energies in the 54 to 117 kJ/mol range for nut pine (*Pinus pinea*) and cork oak (*Quercus suber*) chars, while Tomé et al. [12] got values in the 56.6 and 169.3 kJ/mol range for chars made

with african woods (*Azelia quanzensis*, *Milletia stuhlmannii* and *Pterocarpus angolensis*). Pereira and Pinho [14] obtained values in the 39 to 121 kJ/mol range, for holm oak (*Quercus ilex*), eucalyptus (*Eucalyptus globulus*), maritime pine (*Pinus pinaster*) e cork oak (*Quercus suber*) chars. Janse et al. [35]. present a large set of data collected from the literature from different authors and refer activation energies from 84.9 to 160 kJ/mol for several types of wood chars. Adánez et al. [36] using a modified Arrhenius equation got values in the 55 to 63 kJ/mol range for pine and eucalyptus chars.

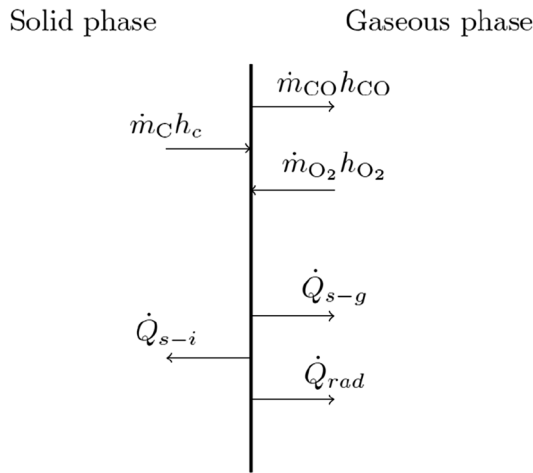


Fig. 11 Energy balance at the surface of the burning particle [34]

components, specially alkaline-earth and non-metallic ones like phosphorus, might have an important impact upon the temperature evolution of the reaction rate constant [20].

Conclusions

In this study on the bubbling fluidized bed combustion of chars, made from vine and kiwi agricultural pruning wastes, and gorse forest residues, it was found that the combustion depends on both, the particle external diffusion process and the heterogeneous phase reaction kinetics, for the kiwi and vine chars. For the gorse char the combustion is purely controlled by the diffusion process.

The activation energy values, 246.16 kJ/mol for the kiwi char and 155.02 kJ/mol for the vine char, are on the high side of the activation energy value ranges, obtained

Table 6 Average temperatures of the char burning particles and corresponding heterogeneous phase reaction rate constants

T_{bed} [K]	Kiwi			Vine			Gorse		
	T_p [K]	ΔT [K]	k_c [ms^{-1}]	T_p [K]	ΔT [K]	k_c [ms^{-1}]	T_p [K]	ΔT [K]	k_c [ms^{-1}]
1023.15	1086.93	63.78	0.2343	1080.57	57.42	0.1979	1085.07	61.92	0.6096
1093.15	1146.12	52.97	0.2733	1142.23	49.08	0.2669	1151.01	57.86	∞
1123.15	1177.22	54.07	1.5639	1169.73	46.58	3.3955	1177.78	54.63	∞
1173.15	1223.56	50.41	4.2617	1221.73	48.58	0.8774	1224.17	51.02	∞

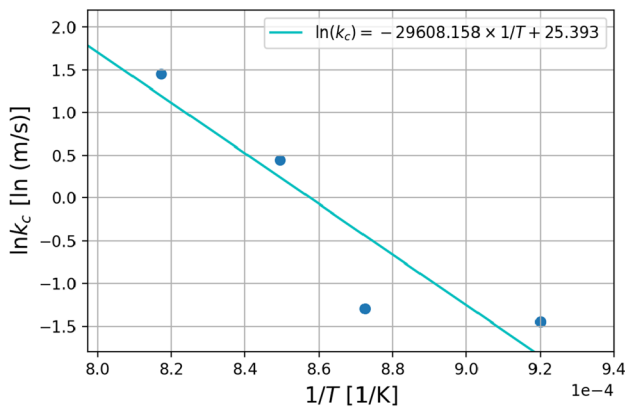


Fig. 12 Arrhenius fitting for kiwi char

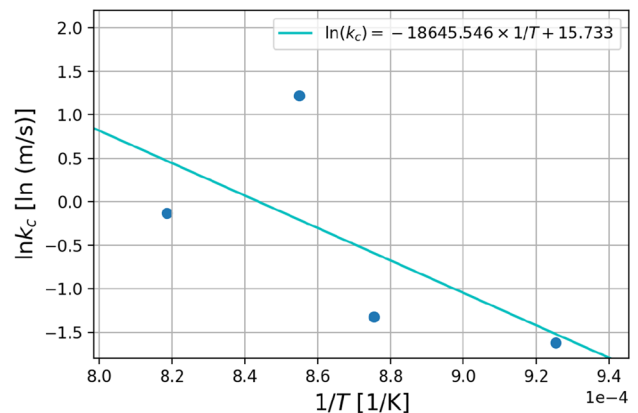


Fig. 13 Arrhenius fitting for vine char

However, the activation values obtained on the present study are on the high side, especially for vine char, being slightly above the values obtained from the majority of the studies that were cited. The vine data, Fig. 13, show some discrepancies towards the straight fitting line, as opposed to the kiwi char. Looking at the higher ash content of the vine char and, compared to the kiwi char, the minor ash

Table 7 Activation energy and pre-exponential factor for kiwi and vine chars

Species	y-intercept	slope	A [$m s^{-1}$]	E_a [$kJ mol^{-1}$]
Kiwi	25.393	-29,608.2	1.06E+11	246.16
Vine	15.733	-18,645.5	6.80E+06	155.02
Gorse	-	-	-	-

in several other studies for wood chars. In the scientific literature there are not available such activation energy values for agricultural wastes, as is the case of the kiwi and vine pruning wastes chars.

Another important conclusion to report here, is that the influence of the particle non-sphericity must be clearly accounted for, otherwise, wrong conclusions concerning the dominating mechanism of the char combustion can be drawn, and supposition of a pure kinetic combustion control could appear. The present work is in line with the interest of agro-forestry residues as an energy source, and how the study of combustion problems arising from some of the minor ash components of these biomasses [23, 37], is becoming an important request for the understanding of the phenomena occurring inside the reaction zone.

Acknowledgements The present work was supported by the INTERREG Project N. PR321705—BIOMASA_AP and carried out in the Combustion Laboratory of INEGI.

References

- Moreira, D., Ferreira, V., Resende, P.R., Pinho, C.: Determination of kinetic data through the fluidized bed combustion of chars made from vine and kiwi pruning wastes. *Energy Rep.* **6**, 615–619 (2020)
- Wolf, J. P.: Biomass combustion for power generation: an introduction. In: L. Rosendahl, (ed), *Biomass Combustion Science, Technology and Engineering*, Chap. 1, p. 3–8. Woodhead Publishing, Oxford, UK (2013)
- Mandø, M.: Direct combustion of biomass. In: L. Rosendahl, (ed), *Biomass Combustion Science, Technology and Engineering*, Chap. 4, p. 61–83. Woodhead Publishing, Oxford, UK (2013)
- Van Loo, S., Koppejan, J.: *The Handbook of Biomass Combustion and Co-firing*. Earthscan, UK (2008)
- Dermibas, K., Sahin—Dermibas, A.: Compacting of biomass for energy densification. *Energy Sour. Part A* **31**, 1063–1068 (2009)
- Dermibas, A., Dermibas, M.F.: Biomass and wastes: upgrading alternative fuels. *Energy Sour.* **25**, 317–329 (2003)
- Basu, P.: *Combustion and gasification in fluidized beds*. Taylor and Francis Group, LLC, London (2006)
- Mazza, G.D., Soria, J.M., Gauthier, D., Urrutia, A.R., Zambom, M., Flamant, G.: Environmental friendly fluidized bed combustion of solid fuels: a review about local scale modeling of char heterogeneous combustion. *Waste Biomass Valor.* **7**, 237–266 (2016)
- Rangel, N., Pinho, C.: Considerations on experimental studies of vegetable char combustion in fluidized bed. *Int J. Energy Clean Environ.* **10**(1–4), 203–215 (2009)
- Rangel, N., Pinho, C.: Kinetic and diffusive data from batch combustion of wood chars in fluidized bed. *Biomass Bioenerg.* **35**(10), 4124–4133 (2011)
- Rangel, N., Pinho, C.: Fragmentation effects on batches of pine wood char burning in a fluidized bed. *Energy Fuels* **24**, 318–323 (2010)
- Tomé, N., Rangel, N., Pinho, C.: Reactivity of biomass chars from mozambique in a fluidized bed combustor. *Int. Rev. Chem. Eng. (IRECHE)* **5**(2), 121–125 (2013)
- Ramos, M., Rangel, N., Pinho, C.: Fluidized-bed combustion of selected wood chars from the semi-arid northeastern region of Brazil. *Energy Fuels* **26**, 400–406 (2012)
- Pereira, C., Pinho, C.: Determination of fluidized bed combustion kinetic and diffusive data of four wood chars from the central region of Portugal. *Energy Fuels* **27**, 7521–7530 (2013)
- Pereira, C., Pinho, C.: Influence of particle fragmentation and non-sphericity on the determination of diffusive and kinetic fluidized bed biochar combustion data. *Fuel* **131**, 77–88 (2014)
- Ferreira, T., Marques, E., Almeida, D., Pereira, C., Paiva, J.M., Pinho, C.: Monitoring Fluidization Quality and Combustion Efficiency of Invasive Species Pellets. 15th Brazilian Congress of Thermal Sciences and Engineering - ENCIT2014, 10 to 13 November, Belém, PA, Brazil (2014)
- Pinho, C., Ferreira, T., Marques, E., Almeida, D., Pereira, C., Paiva, J.M.: Obtaining Diffusive and Kinetic Data from Batch Combustion of Invasive Species Char Pellets. 15th Brazilian Congress of Thermal Sciences and Engineering - ENCIT2014, 10 to 13 November, Belém, PA, Brazil (2014)
- Pinho, C., Ferreira, T., Pereira, C., Paiva, J. M.: Combustion of Invasive Acacia Dealbata Char Pellets – Determination of Diffusive and Kinetic Data. 23rd ABCM International Congress of Mechanical Engineering – COBEM 2015, 6 to 11 December, Rio de Janeiro, RJ, Brazil (2015)
- Marques, E., Pereira, C., Paiva, J., Pinho, C., Ferreira, T.: Fluidized bed combustion of char pellets made from blends of shrubs and cork residues. 24th ABCM International Congress of Mechanical Engineering- COBEM 2017, 3 to 8 December, Curitiba, Pr, Brazil (2017)
- Pereira, C., Pinho, C.: Analysis of the fluidized bed combustion behavior of Quercus ilex char. *Appl. Therm. Eng.* **81**, 346–352 (2015)
- Marques, E., Ferreira, T., Pereira, C., Paiva, J.M., Pinho, C.: Analysis of kinetic and diffusive data from the combustion of char pellets made with hybrid mixtures. *Energy* **181**, 1179–1188 (2019)
- Verma, D., Fortunati, E., Jain, S., Zhang, X.: Biomass, biopolymer-based materials, and bioenergy. construction, biomedical, and other industrial applications. (eds.). Woodhead Publishing, UK (2019)
- Niu, Y., Tan, H., Hui, S.: Ash-related issues during biomass combustion: Alkali-induced slagging, silicate melt-induced slagging (ash fusion), agglomeration, corrosion, ash utilization, and related countermeasures. *Prog. Energy Combust. Sci.* **52**, 1–61 (2016)
- The Spyder Website Contributors: spyder the scientific python development environment. <https://www.spyder-ide.org/> Accessed 28 May 2018
- Riaza, J., Gibbins, J., Chalmers, H.: Ignition and combustion of single particles of coal and biomass. *Fuel* **202**, 650–655 (2017)
- Wang, Q., Zhao, W., Liu, H., Jia, C., Xu, H.: Reactivity and kinetic analysis of biomass during combustion. *Energy Procedia* **17**, 869–875 (2012)
- Neves, D., Matos, A., Tarelho, L., Thunman, H., Larsson, A.: Volatile gases from biomass pyrolysis under conditions relevant for fluidized bed gasifiers. *J. Anal. Appl. Pyrol.* **127**, 57–67 (2017)
- Hesketh, R.P., Davidson, J.F.: The effect of volatiles on the combustion of char in a fluidised bed. *Chem. Eng. Sci.* **46**, 3101–3113 (1991)
- Ribeiro, L., Pinho, C.: Generic behaviour of propane combustion in fluidized beds. *Chem. Eng. Res. Des.* **82**, 1597–1603 (2004)
- Pinho, C.: Fragmentation on batches of coke or char particles during fluidized bed combustion. *Chem. Eng. J.* **115**, 147–155 (2006)
- Ferreira, T., Pereira, C., Paiva, J.M., Pinho, C.: Simple methodology to quantify the fragmentation on batches of char pellets during fluidized bed combustion. *Energy Fuels* **31**, 5073–5078 (2017)
- Ross, I.B., Davidson, J.F.: The combustion of carbon particles in a fluidized bed. *Trans. Inst. Chem. Engrs.* **59** (1981)
- Avedesian, M.M., Davidson, J.F.: Combustion of carbon particles in a fluidised bed. *Trans. Inst. Chem. Engrs.* **51**, 121–131 (1973)

34. Tomé, N., Rangel N., Pinho, C.: Temperature of wood char particles burning in a fluidized bed reactor. *Renew. Energy Power Qual. J. (RE&PQJ)* **10**, (2012)
35. Janse, A.M.C., De Jonge, H.G., Prins, W., Van Swaaij, W.P.M.: Combustion kinetics of char obtained by flash pyrolysis of pine wood. *Ind. Eng. Chem. Res.* **37**(10), 3909–3918 (1998)
36. Adánez, J., de Diego, L.F., García-Labiano, F., Abad, A., Abanades, J.C.: Determination of biomass char combustion reactivities for FBC applications by a combined method. *Ind. Eng. Chem. Res.* **40**(20), 4317–4323 (2001)
37. Yuan, R., Yu, S., Shen, Y.: Pyrolysis and combustion kinetics of lignocellulosic biomass pellets with calcium-rich wastes from agroforestry residues. *Waste Manage.* **87**, 86–96 (2019)

Publisher's Note Springer Nature remains neutral with regard to jurisdictional claims in published maps and institutional affiliations.